HIDRA Mission Report
Analysis of Rural Human Development on Surrounding Environments

John P. McCulloch, Bradley Karas, Jacob Trahan, Nijiel Rocha, and Akshay Vijay

School of Earth and Space Exploration, Arizona State University, Tempe, Arizona

December 9, 2016

The Urban Heat Island effect (UHI) is an established phenomenon where urban centers, due to concrete, pavement, power structures, and the like generate and retain more heat than their surrounding undeveloped environments. The HIDRA (High-altitude Infrared Device for Research and Analysis) mission's primary objective was to study the effects of human development on rural environments by taking thermal images in the 7μm - 13μm range and comparing the areas surrounding developed land to similar non-developed land. In order to collect data, the HIDRA payload consisted of a thermal infrared camera and a visual camera. Of the images collected at float altitude, only a fraction of them were not mostly obscured by clouds and therefore useful for analysis. Of these images, only a few contained developed areas. Contour and heat maps were created from the infrared images and an attempt at calibrating them was made. Technical issues with the camera preventing exposure and shutter control led to high levels of noise and questions about accuracy. From the data obtained, though, the surrounding terrain was approximately 2C or more warmer than the manmade structures and farm land. Based on these results, it is suggested that further research be done to investigate rural human development on the surrounding environment.

Contents

Introduction

It is understood from previous studies that human development on a large scale can cause changes in the surrounding environments. The Urban Heat Island effect (UHI) is one such example. UHI refers to how the surface temperature of an urban area is warmer than the surrounding rural areas. This is due to factors such as urban infrastructure (ex. Dark roofs that absorb and retain heat) and heat generated by automobiles, industries, and population density. A study by Dousset et al. (2010) used maps from the United States Geological Survey's (USGS) Landsat satellite and land surface temperature data from the Moderate-resolution Infrared Spectroradiometer to quantify the Urban Heat Island effect. However little has been done to study the effects of the human-environment interaction on the smaller, rural scale.

Therefore, the primary scientific objective of the HIDRA mission was study the effects of human development on rural environments by taking thermal images in the 7μm - 13μm range and comparing the areas surrounding developed land to similar non-developed land. In the hope of developing a preliminary understanding of the human-environment interaction on the rural scale and potentially making the case for future study.

Objective	Measurement	Measurement Requirements	Instrument	Instrument Requirements	Data Products
Understand the effects of "UHI" on a rural scale by measuring surface temperature at float altitude	Thermal Infrared Image	Image using the 9.3 - 12.4 um infrared wavelength range 70m resolution 3 images of the same object	IR camera	35m/pixel @ 36 km altitude <0.5 pixel smear at 36 m/s and 36 km altitude	image
	Visual Image	70m resolution 3 images of the same object	Visual camera	35m/pixel @ 36 km altitude <0.5 pixel smear at 36 m/s and 36 km altitude	image

Figure 1: Science traceability matrix

To complete these scientific objectives, the above was required of the HIDRA system. (**Figure 1**) The wavelength requirements for the thermal infrared camera were determined by using the information regarding the minimum and maximum expected temperatures of the various environments that HASP could encounter and finding their minimum and maximum emittance wavelengths for those temperatures. (**Figure 2**) The spectral band listed in **Figure 1** coincides with the peak infrared wavelengths of the maximum and minimum temperatures listed in **Figure 2**.

Environment	T_{max} (^{o}C)	T_{min} (^{o}C)	$\lambda(T_{max})$ (μm)	$\lambda(T_{min})$ (μm)
Coniferous Forest	-40	20	9.885	12.428
Deciduous Forest	-30	30	9.559	11.917
Desert	-3.9	38	9.313	10.762
Grassland	-20	30	9.559	11.447

Figure 2: Temperature range and corresponding infrared wavelength of the potential environments encountered during flight.

The resolution requirement for the thermal infrared camera was set to 70m as this resolution was small enough for the camera to resolve large urban structures and parking lots, farming plots, and fields. In order to resolve a 70m area, a minimum of two pixels are needed therefore set infrared camera must have a resolution of 35 m/pixel or better at an altitude of 36 km which is the expected float altitude for HASP. Finally, the infrared camera must have a shutter speed fast enough to prevent image smear at float altitude of 36 km. Since the expected speed for the HASP gondola at 36 km is approximately 36 m/s in speed over the ground, the camera must have less than 0.5 pixels of smear. The requirements for the visual camera are not as strict as those for the thermal infrared camera as the visual camera is only used for help in identifying what is in the thermal image.

HIDRA Payload Description

The HIDRA aluminum structure was bolted to the supplied pvc mounting plate and subsequently attached to an outer arm of the HASP gondola. HIDRA was supplied 28-33 VDC from HASP though an EDAC 516 connection imbedded in the mounting plate. Additionally imbedded in the mounting plate was a DB9 serial connection.

The direct current supplied by HASP was routed through the EDAC 516 connection to the HIDRA payload where it was stepped down to 5 VDC through a DC-DC converter. The DC-DC converter then output the 5 VDC to the Raspberry Pi CPU and to the FLIR camera through a time delay switch. Turning the system on and then the FLIR reduced the in-rush current to levels well beneath the 500 mA limit of the HASP fuses. The Raspberry Pi CPU was further connected to and supplied powered to the following components: Labjack U3, Raspberry Pi camera, 64GB USB flash drive, GPIO-Serial converter module, and the trigger pin on the time delay switch.

The purpose of the Labjack was to command and control the FLIR camera via the PWM port on the FLIR camera. To do so, the Labjack generated a PWM signal at 3.3V, 50Hz where the “Low” classification was characterized as a 5% duty cycle, and the “High” classification characterized by a 50% duty cycle. Sending the “High” state signal triggered the FLIR to take a picture. This was done every 60 seconds and then the signal was returned to the “Low” state. The images captured by the FLIR camera were stored internally on a 32GB SD card in the FLIR camera module. To obtain visual images, the Raspberry Pi CPU was connected to a Raspberry Pi camera via a CSI port and took images every 60 seconds to match with the thermal images captured by the FLIR. The visual images were stored on the 64GB flash drive.

Additionally, the Labjack was connected to three temperature sensors which receive power directly from the DC-DC converter via a breadboard with resistors inline and the outputs of the temperature sensors are read by the Labjack and converted from Kelvin to Fahrenheit when stored and transmitted. These three temperature sensors were placed on the FLIR camera, the aluminum frame, and the DC-DC converter to ensure that none of the components were exceeding their maximum or minimum operating temperatures. The Labjack also recorded and transmitted its own internal temperature.

Finally, HIDRA communicated with HASP and the ground crew over serial. The Raspberry Pi CPU connected via GPIO to a serial converter which then ran through a null adapter to the mounting plate serial port which was connected to HASP. Communication consisted of data packets transmitted every 60 seconds and allowed the ground crew to monitor HIDRA’s status during flight to ensure it was functioning properly.

The description of the system above is that of the system that took flight. This system did have deviations from the original design as detailed below.

- The original design incorporated much smaller DC-DC converters, however it was found that these smaller ones could not sustain reliable power at high temperatures or low pressures. Thus

the the new larger ones with heat syncs were incorporated. When the idea of installing the time delay switch came about, it was determined that two DC-DC converters were unnecessary and one was removed to make space inside the aluminum structure for the time delay switch. (Removing one of the DC-DC converters also lead to the removal of the temperature sensor that was affixed to it.)

- The original design's power system had a set of three current sensors. However, in subsystem testing and integration, it was determined that the current sensors produced a significant amount of noise in the system and prevented the FLIR camera from triggering properly. All three were removed from the system to reduce the noise and system power performance was monitored through the HASP current readings.
- The original design did not have the time-delay switch incorporated in it. However, in lab tests it was noticed that when the system turned out there was a large in-rush current spike that exceeded the HASP fuse specifications. The time-delay switch was installed to turn everything but the FLIR camera on first, then after a period of time, turn the FLIR camera on. This reduced the in-rush current immensely and brought it well below the fuse specifications.

Data and Data Collection

There are three main categories of data collected by HIDRA during flight: thermal images, visual images, and telemetry data. The thermal image category consists of the 1,061 infrared images in the 7.5µm to 13.5µm range. The FLIR camera used to take these images stored them on its internal microSD card as 14 bit tiff images. These "raw" images were then converted to standard 16 bit tiff images. Once all of the images were converted to 16 bits, a plot of the maximum and minimum pixel value from each image. Since the images were taken sequentially each minute during flight operations, the graph becomes a plot of maximum and minimum pixel value over time for the duration of the flight. (**Figure 16**) The thermal images taken while at float comprise the primary data set for analysis.

The principal motivation behind collecting the visual images was to match each visual image up to it corresponding thermal image to provide the context of land cover found in the thermal image. Even though the visual camera had a slightly larger field of view, geographic and land cover features from each visual image could be found easily in the thermal image allowing for each thermal image to be classified. These images were stored on the Raspberry Pi's external flash drive.

The final data category is the telemetry data and was collected by HIDRA or by HASP. The HIDRA system collected and stored the following data: the number of times the FLIR camera was triggered, the number of visual images taken by the Raspberry Pi camera, temperature sensor measurements of the three components listed above, and the Labjack's internal temperature. Not only was this data stored as a text file on the Raspberry Pi's external flash drive, but was also transmitted via the serial connection from the HIDRA system to the ground crew. (**Figure 3**) This data was primarily used to monitor the HIDRA system while in flight and ensure that no components exceeded their temperature ranges and that the system was still taking pictures. The count of the thermal images would reset if the system ever restarted which would allow the ground crew to know if the system had power cycled. **Figure 4** is a plot of the four temperatures over time during flight.

nFLIR	nVis	tempFLIR	tempRPi	tempFrame	tempLabjack
216	216	11.8136	25.7979	53.1246	30.2867
217	217	12.8893	25.7979	54.2004	31.0035
218	218	11.8136	26.8736	55.2761	31.7204
219	219	12.8893	25.7979	55.2761	32.4373

220	220	12.8893	26.8736	55.2761	33.1542

Figure 3: HIDRA system telemetry readings at the start of float. Temperatures are in Celsius.

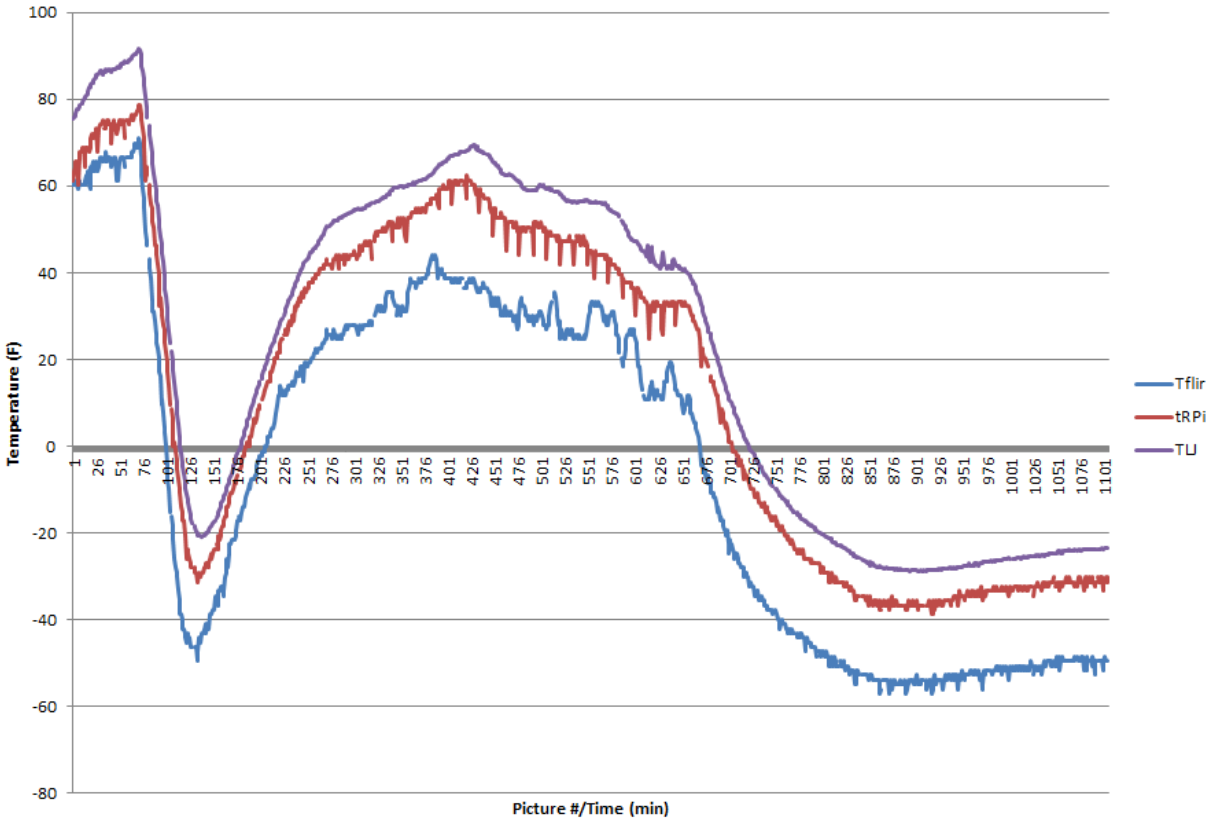

Figure 4: Plot of component temperature over time in degrees Celsius. Where Tflir is the temperature of the FLIR Camera measured by a temperature sensor, tRPi is the temperature of Raspberry Pi measured using a temperature sensor, and TLJ is the temperature of the Labjack measured by its internal temperature sensor.

In addition to the data collected by the HIDRA system, HASP also provided voltage and current readings via their website. The ground crew was able to use this data to determine if HIDRA was functioning properly. As long as the voltage readings remained in the range of the HASP supply, the crew knew that HIDRA was powered on. Based off the current readings, the HIDRA team could tell what the system was doing when the measurement was made. If the current read between 170mA and 190mA the system was on and in a rest period between taking images. If the measurement was between 210mA and 230mA, the measurement had been taken while the FLIR camera was taking a picture or calibrating. As long as the current readings showed a couple of the 210mA to 230mA measurements dispersed among the 170mA and 190mA, HIDRA was functioning normally. **Figure 5** is a plot of HIDRA's voltage and current readings over time. By all indications from the data sets collected it appears that the HIDRA mission had a smooth flight and performed as designed.

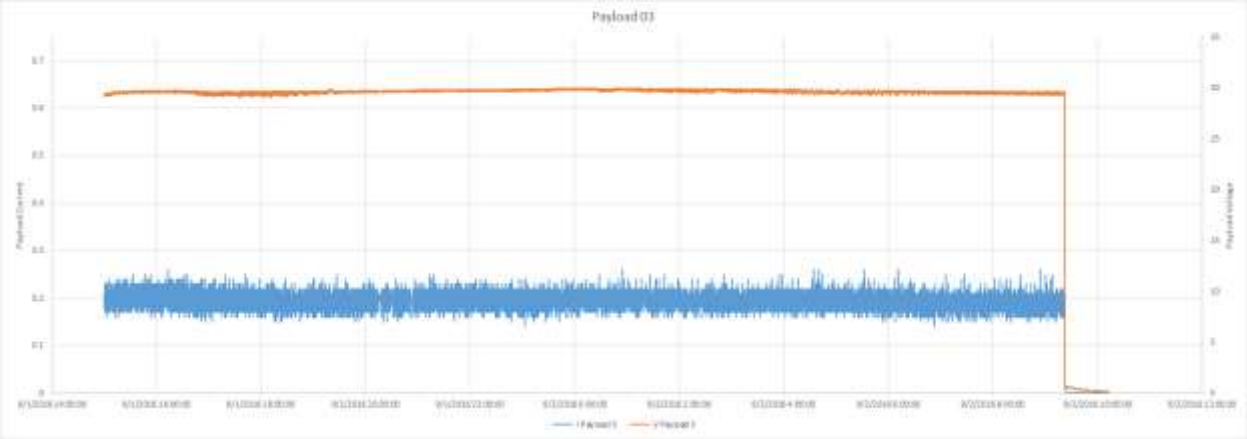

Figure 5: Voltage (orange) and current (blue) measurements of the HIDRA payload during flight.

Data/Image Analysis Methods

The preliminary step in image analysis was to determine which images were collected at float altitude, as these are the images that the analysis is focused on. This was done by finding the first image taken during launch (IR0072) and matching it up with the HASP recorded time of launch (16:08 UTC). Due to the HIDRA imaging rate of one picture every minute, each additional minute corresponds to the next picture. HASP reached float altitude at 18:32 UTC for a total of 144 minutes of ascend time. Since launch is cataloged by IR0072, images at float begin at IR0216 (72+144=216). The last image of the analysis range was determined using two different methods. The first was to qualitatively look through each image and determine where the visual images become too dark to identify anything in and was catalogued at IR0633. The other method was to plot the maximum and minimum pixel values and determine where there were was a drastic decrease, indicative of nightfall, and mark that as the end of the analysis range. This method catalogued the last analysis image as IR0687. It was decided that IR0633 would be the terminus of the analysis range as visually inspecting images past IR0633 proved too difficult to determine what was in them. With the range of IR0216 to IR0633 yields a total number of images of 417.

The infrared images within the analysis range were matched up with the corresponding visual images collected by the Raspberry Pi camera. Using these side-by-side images, each land cover category found in the image was identified qualitatively based off the following definitions from the USGS NLCD 92. (**Figure 6** shows the classifications that were identified in the images.) Due to precipitation in the launch area and along the flight path, 228 of the images taken at float altitude were discarded because the majority of the image was obscured by cloud cover. The remaining images were then narrowed down to the set containing features that were man-made.

ID#	Name	Description
11	Open Water	All areas of open water, generally with less than 25% cover of vegetation/land cover.
21	Low Intensity Residential	Includes areas with a mixture of constructed materials and vegetation. Constructed materials account for 30-80 percent of the cover. Vegetation may account for 20 to 70 percent of the cover. These areas most commonly include single-family housing units. Population densities will be lower than in high intensity residential areas.
23	Commercial, Industrial, Transportation	Includes infrastructure (e.g. roads, railroads, etc.) and all highly developed areas not classified as High Intensity Residential.

31	Bare Rock, Sand, Clay	Perennially barren areas of bedrock, desert pavement, scarps, talus, slides, volcanic material, glacial debris, beaches, and other accumulations of earthen material.
33	Transitional	Areas of sparse vegetative cover (less than 25 percent of cover) that are dynamically changing from one land cover to another, often because of land use activities. Examples include forest clearcuts, a transition phase between forest and agricultural land, the temporary clearing of vegetation, and changes due to natural causes (e.g. fire, flood, etc.).
81	Pasture, Hay	Areas of grasses, legumes, or grass-legume mixtures planted for livestock grazing or the production of seed or hay crops.
83	Small Grains	Areas used for the production of graminoid crops such as wheat, barley, oats, and rice.

Figure 6: NLCD 92 categories and definitions identified in HIDRA images.

Data/Image Analysis

The FLIR camera during testing was found to not support radiometric calibration. However, an attempt was still made for image analysis. The first step involved taking a series of images of a simulated blackbody that was heated using a heat gun and permitted to cool back down to room temperature. The temperature of the blackbody was recorded with the same temperature sensor that can be found throughout the HIDRA payload. The pictures were taken once a minute to reflect the interval between pictures during flight. An average pixel value for each of the images was found by taking the median value of the pixels that corresponded to the blackbody. These pixel values were then plotted against the recorded temperature to create a calibration curve along with a calculated best fit quadratic line. **Figures 7, 8, 9, and 10** show the data along with the best fit line that were obtained on the two calibration heating trials. An average of the two calculated best fit lines was used as the conversion between the pixel values and a given temperature.

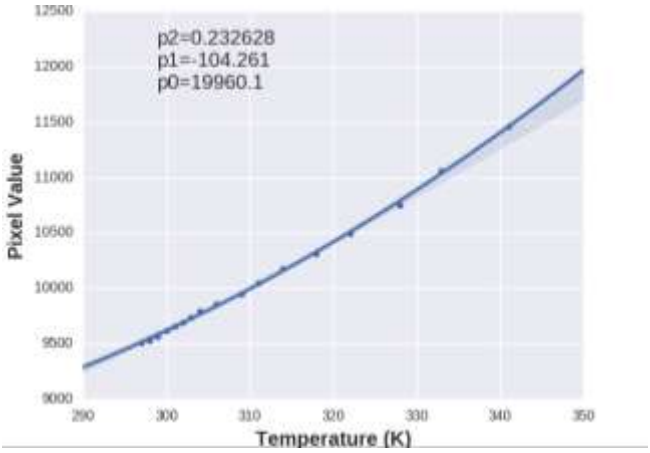

Figure 7: Calibration data for trial 1 of FLIR camera

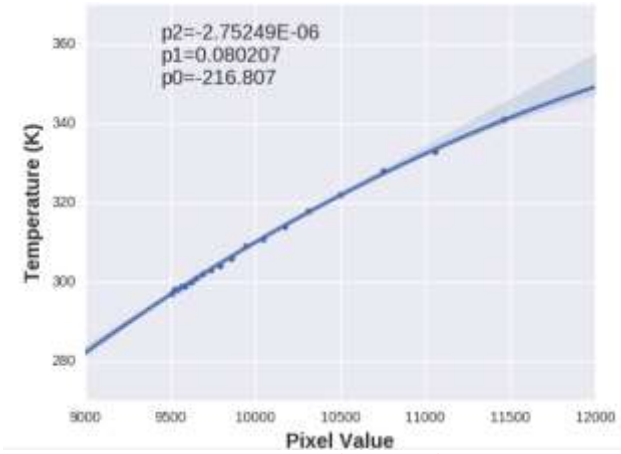

Figure 8: Calibration data for trial 1 of FLIR camera

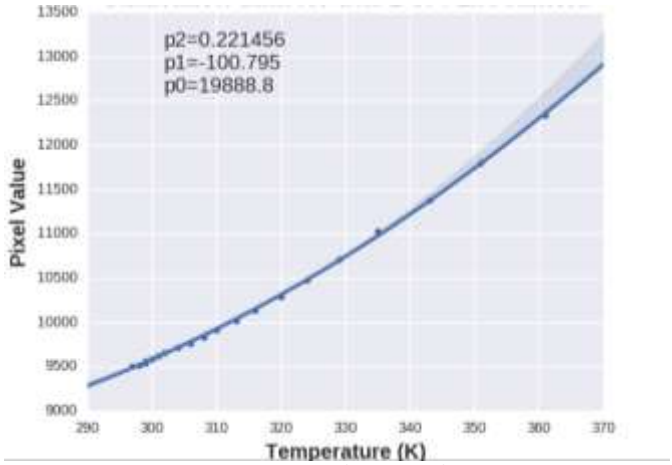

Figure 9: Calibration data for trial 2 of FLIR camera

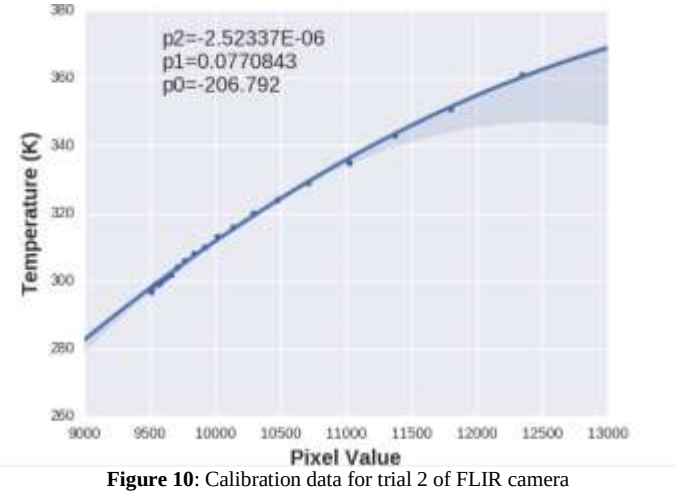

Figure 10: Calibration data for trial 2 of FLIR camera

Flat field images were taken to reduce the pixel to pixel variability in the images. The blackbody was placed inside the focal distance of the camera such that it filled up the entire image. These images were taken at room temperature at a cadence of one per minute. The flats were median combined three at a time to reduce noise. These median combined flats were then averaged to create a master flat image

shown in **Figure 11** with a distribution of the pixel values shown in **Figure 12**. The master flat image was then normalized using the median pixel value from the master flat to create **Figure 13**.

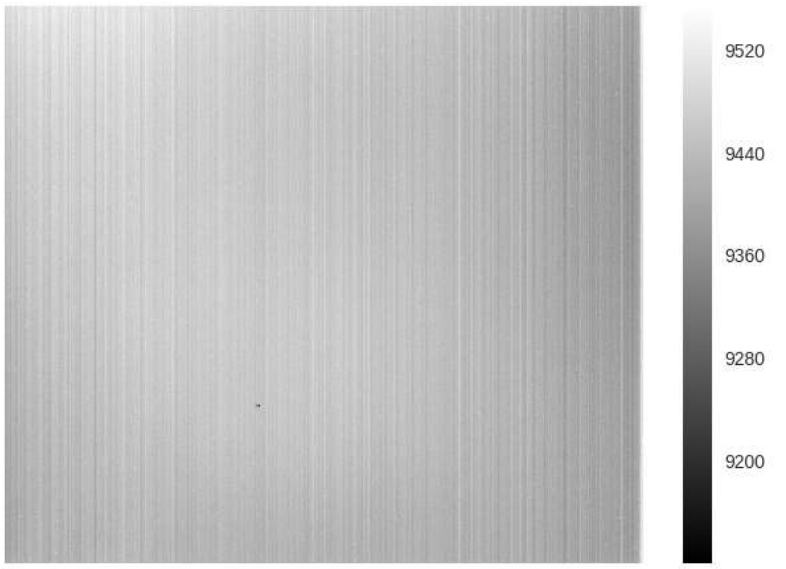

Figure 11: Flat field pixel values

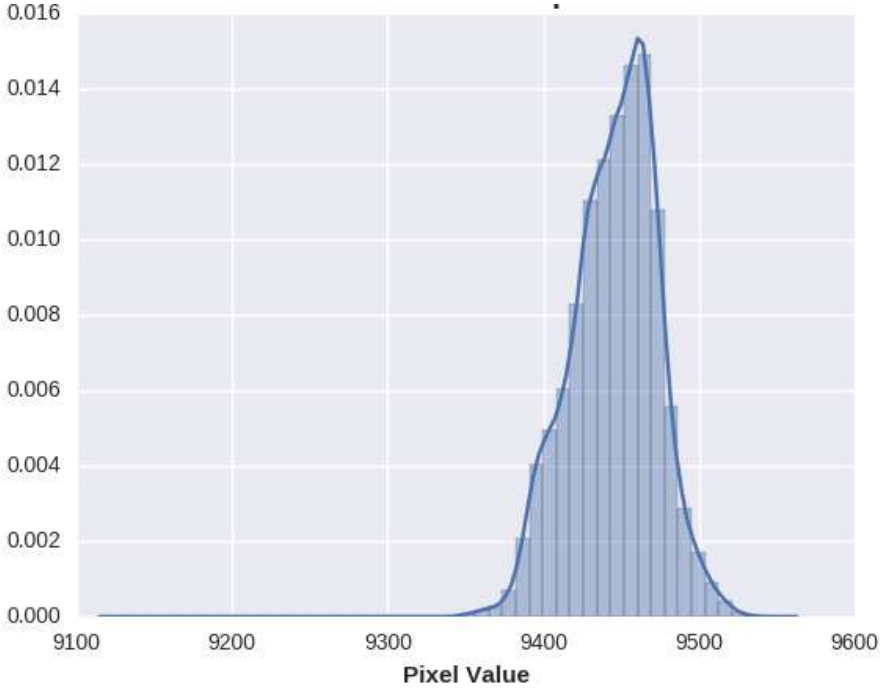

Figure 12: Distribution of flat field pixel values

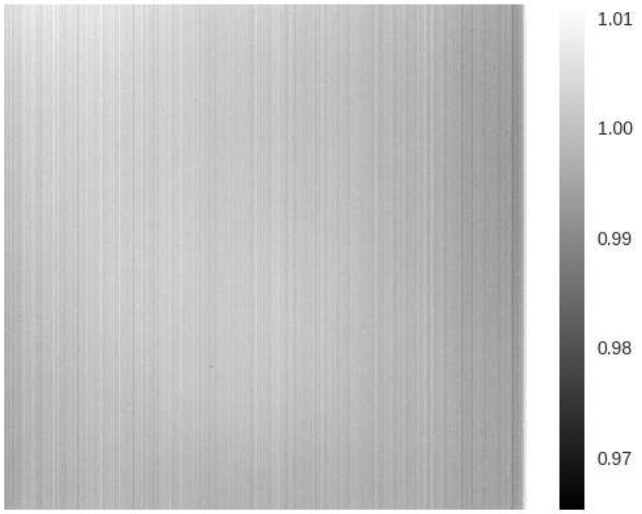

Figure 13: Normalized flat field

Bias and dark frames were not taken. The limitations in the camera interface prevented user control of the shutter and exposure times. This prevented the removal of the bias lines, but was deemed acceptable due to the reduced variability and noise of the images processed with the flats when compared to the unprocessed images.

The maximum, minimum, and mean pixel values for each of the images taken from the flight can be found in **Figure 14**. There were 5 shifts in pixel values between images. The pixel values in the images were shifted to match up with those in the middle, 216 to 633, that corresponded to float during the day. **Figure 15** shows the pixel values after the adjustment.

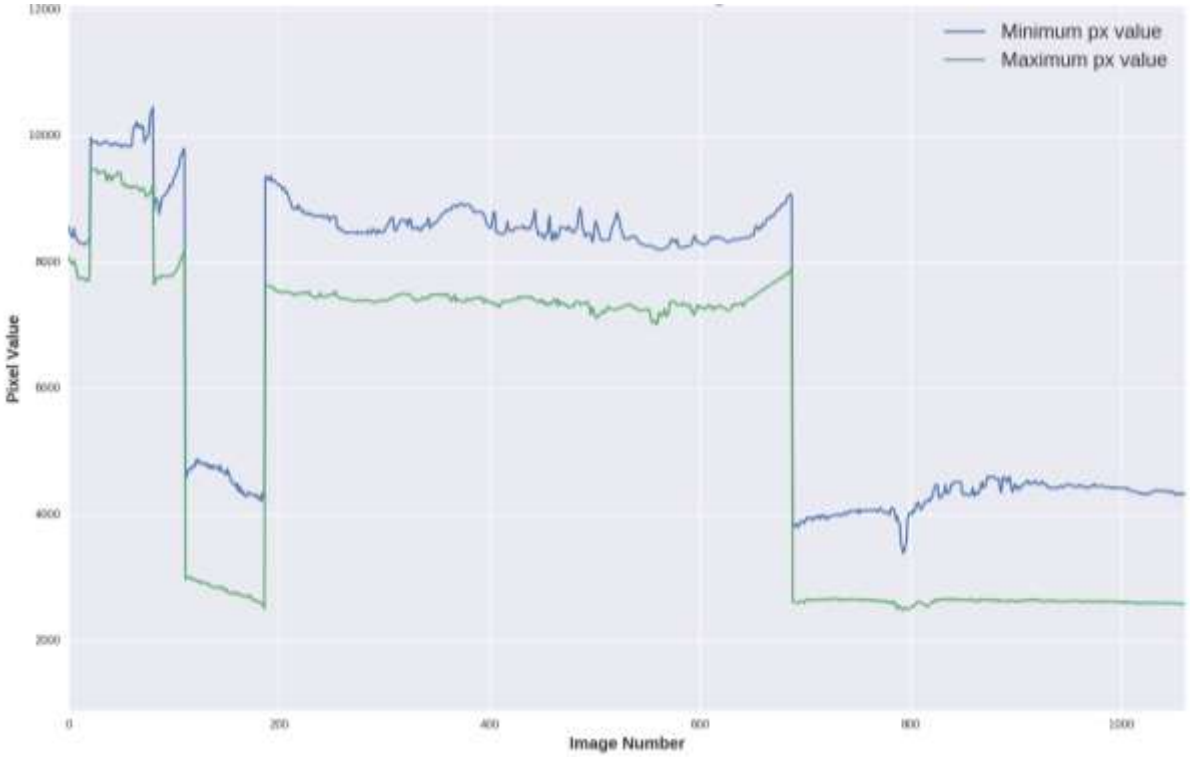

Figure 14: Raw values for IR images

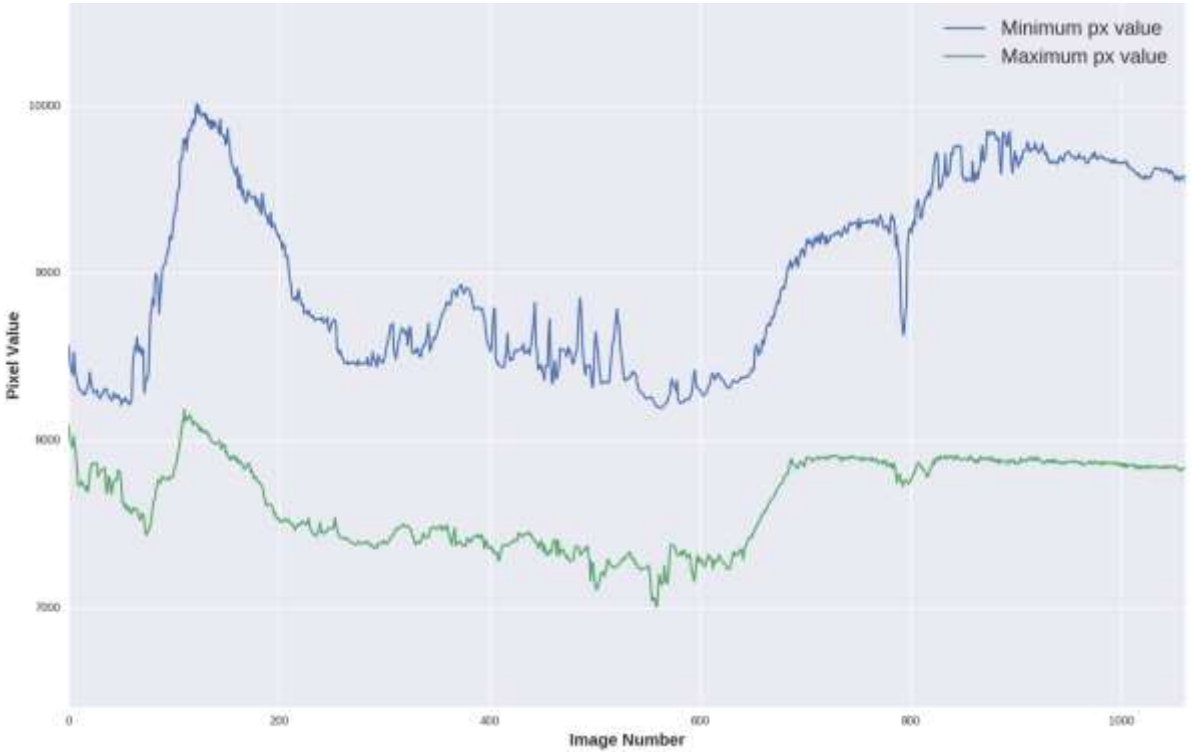

Figure 15: Raw values for IR images adjusted

After the pixel shift adjustment, the images of the tarmac were used to give a rough estimate of the pixel value for the tarmac. The temperature of the tarmac at launch was taken with a heatgun. However, the record of that temperature was lost before analysis began. An estimate of 74.0°F (23.33°C) was used from memory and the project member in charge of the tarmac temperature data was sacked. The pixel number for the tarmac varied and an average number was used of 8150. From the calibration data, the pixel value should have been about 9484.18. Thus, a pixel shift of 1334.18 was applied prior to the application of the calibration curve. The calibration curve below pixel value of 11000 is approximately equal to a linear fit and no flight data contained a pixel value above that. Thus, it was deemed acceptable to use the pixel shift offset as the flight data is contained within the linear portion of the calibration curve. **Figure 16** shows the temperature value ranges for the different images obtained after the calibration and flats were applied.

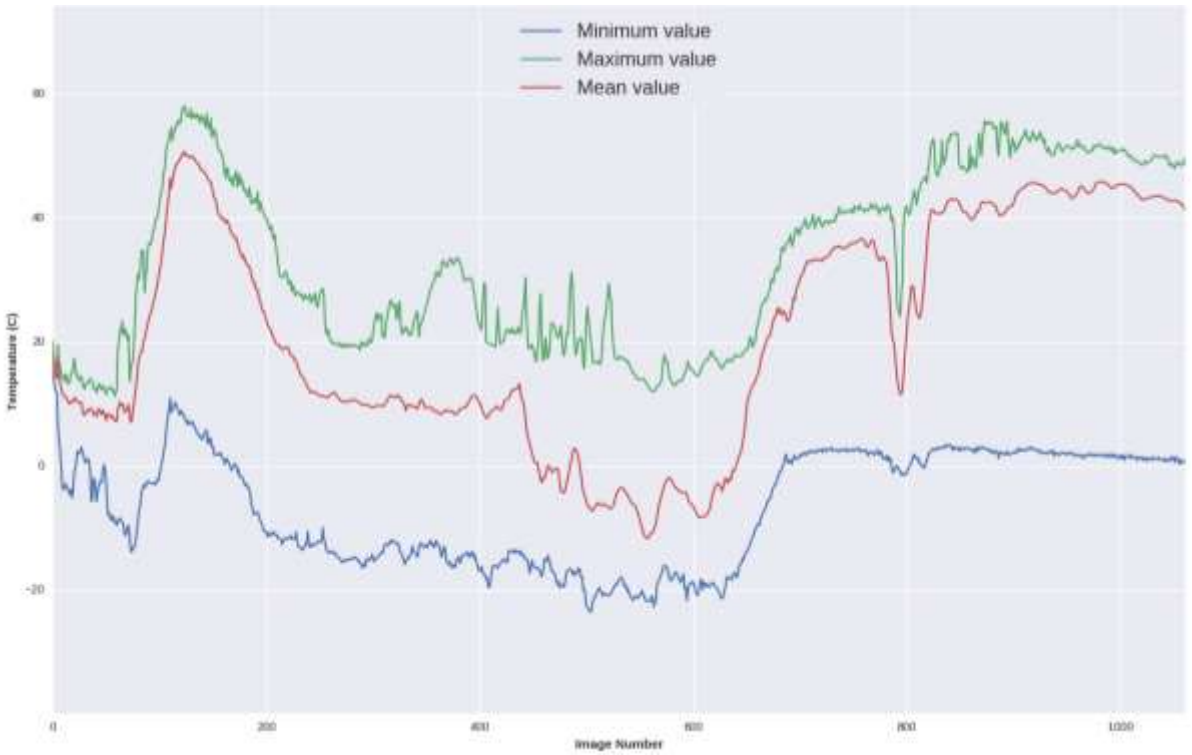

Figure 16: Calibrated values for IR images

The calibrated image data was used to create distribution plots, contour plots, and heatmaps for each of the 1062 images obtained during flight. The contour maps were created with a contour interval of 2℃. The interval was chosen to be the smallest while limiting the visible noise in the contour plots. The images at float during the day, images 216 to 633, were paired up with their complementary visual images. The pairs of images were then analyzed for the types of terrain as discussed above that were visible in both the visible and infrared images. Of those, the majority were mostly or entirely covered in cloud cover. Several, though, had visible terrain.

A good example of an image relatively free of clouds and possessing several of the above land types was image 436 as seen in **Figure 17** of the visual image. The image contains visible roads, housing, agricultural lands, a river, and the surrounding terrain mostly made up of bare rock and dirt. **Figure 18** shows the heatmap of the infrared image with the scale in ℃. **Figure 19** shows the contour map of the corresponding infrared image with the aforementioned contour interval of 2℃ and the contour lines labelled by both color and number. **Figure 20** shows a histogram of the image showing the different temperatures. Interestingly, the surrounding terrain at 30℃ to 32℃ appears warmer than the buildings (26℃) and agricultural land area (24℃). Unfortunately, due to the noise, 2℃ is the smallest difference in temperature that can be measured.

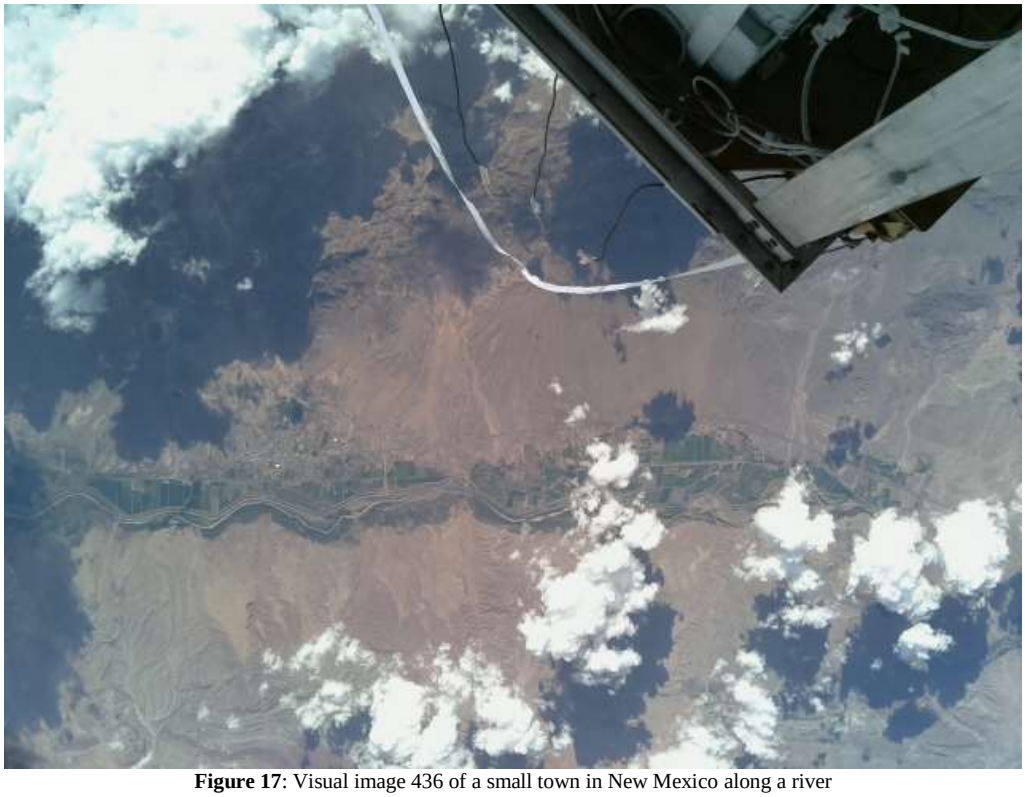

Figure 17: Visual image 436 of a small town in New Mexico along a river

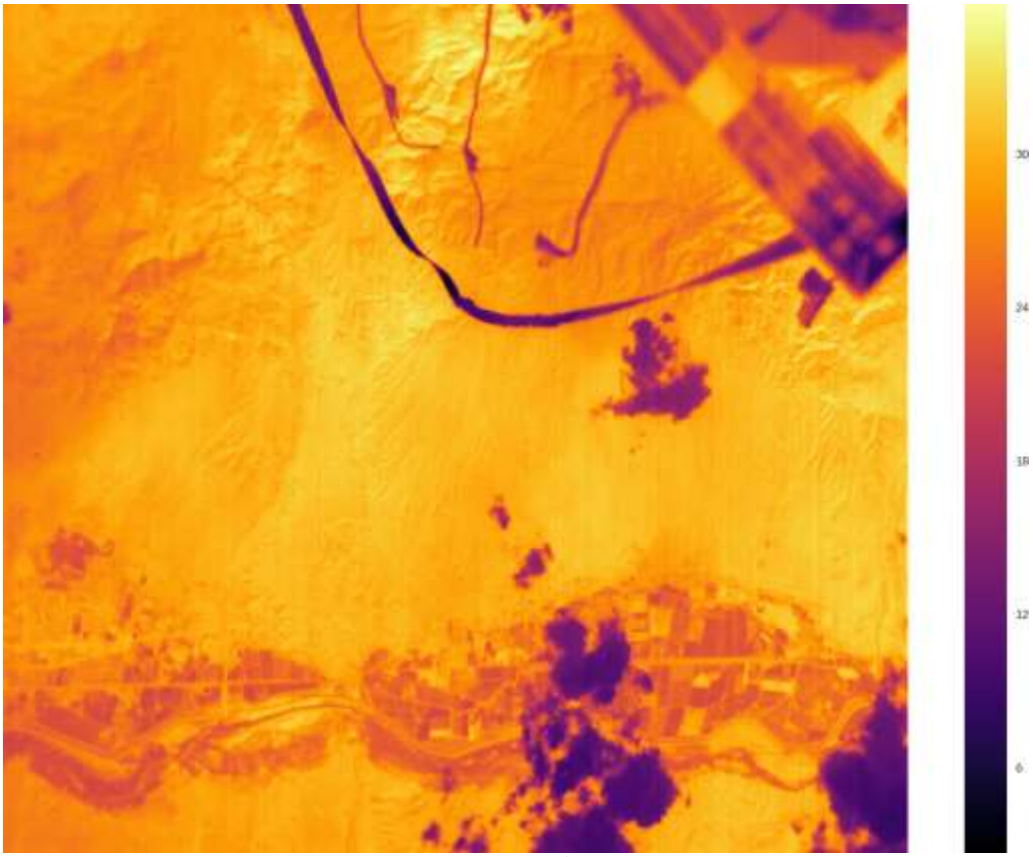

Figure 18: Heatmap of image 436

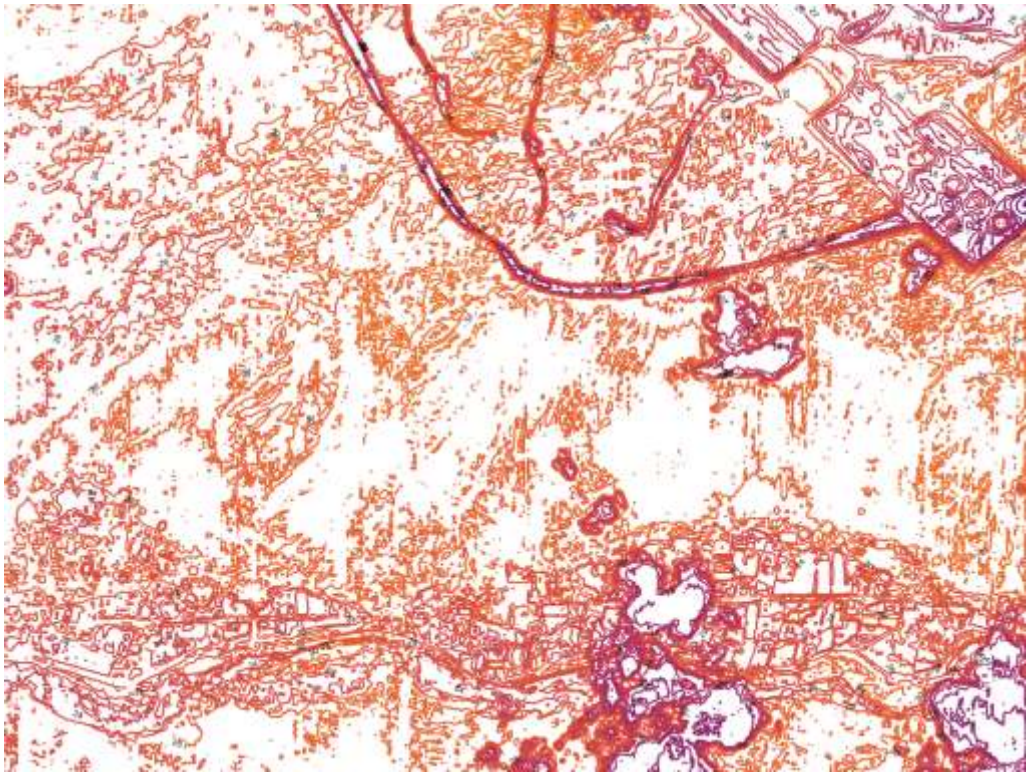

Figure 19: Heat contour map of image 436

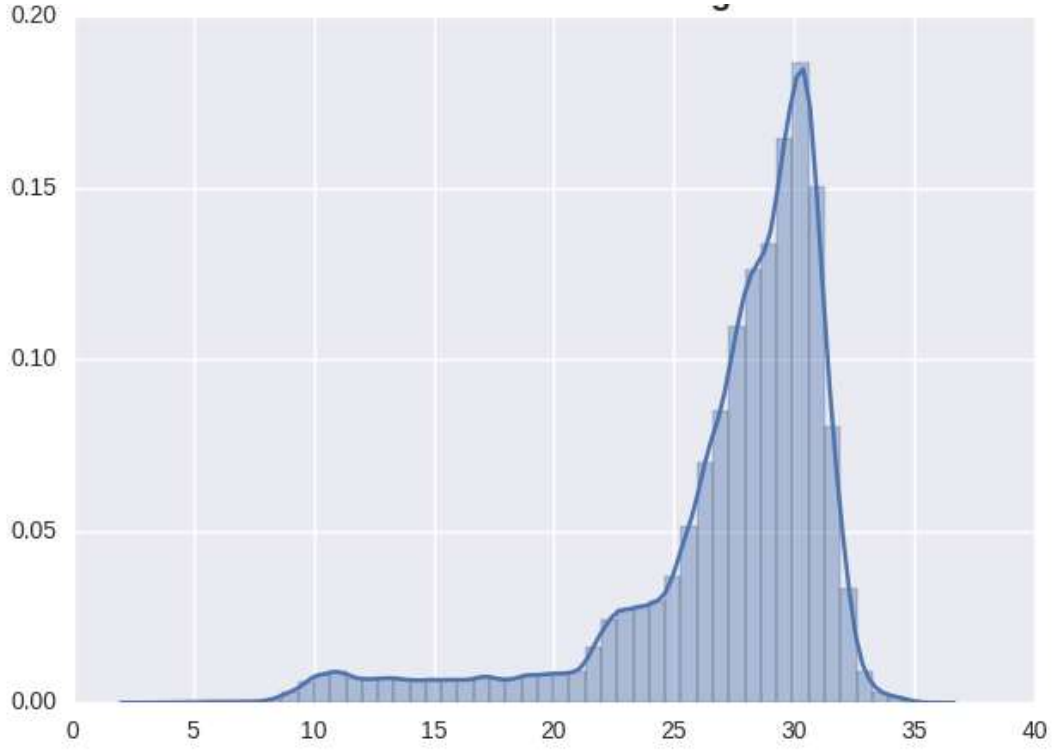

Figure 20: Distribution of values for image 436

Conclusion

The payload was successfully launched and obtained all the required data during flight. A total of 1062 visual and infrared images were taken during flight that included some night time travel. Of those images, a majority of them were covered in clouds. Limitations of the camera were unfortunately not discovered until too late during the testing process. The firmware and related software interface of the camera prevented user control of exposure times and shutter. This prevented proper image analysis calibration images of bias and dark frames from being taken. The camera was also found to be incapable of radiometric calibration as the camera would arbitrarily change the pixel values and exposure times of images based on the temperature of the camera itself. It was thought that the auto-contrast was turned off in the software settings. However, analysis of the image data from flight suggested that it re-calibrated at least 5 times and drastically shifted the pixel values seen in the images. Most likely these were due to the temperature of the camera itself as the images corresponded to flight ascent to float and the onset of night. Despite all of that, a brute force method was devised to obtain some quantitative data from the flight. The combination of noise level and shifting pixel values due to lack of control of the camera prevented accurate quantitative analysis of the images.

Given all of the above, a follow-up study is warranted to obtain the needed resolution of temperature data required for analysis. The project was successful as a technology demonstration showing that we can fly the payload and get data. As a science mission, though, we mostly failed because of limitations in control of the camera settings to reduce noise levels and accurately calibrate the camera. A new camera that allows for radiometric calibration as well as user control of exposure time and shutter control would be required for a successful follow-up science mission.

Team Roles and Demographics

Name	Role	Status	Education	Gender	Ethnicity	Race	Disability
John McCulloch	Project Manager Systems Engineer Power Systems Engineer	Active	Graduate Student	Male	Non-Hispanic	Caucasian	No
Bradley Karas	Mechanical Engineer Camera Systems Engineer Scientific Analysis Lead	Active	Graduate Student	Male	Non-Hispanic	Caucasian	No
Jacob Trahan	Software Engineer Communications Engineer	Active	Undergraduate	Male	Non-Hispanic	Caucasian	No
Nijiel Rocha	Support Engineer - Thermal Systems, Calibration, & Assembly	Active	Post - Undergraduate	Male	Hispanic	Hispanic	No
Akshay Vijay	Support Engineer - Testing & Machining	Active	Undergraduate	Male	Non-Hispanic	Asian Indian	No
Christopher Groppi	Faculty Advisor	Active	Professor	Male	Non-Hispanic	Caucasian	No
Andrew Thoeson	Graduate TA	Inactive July ‘16	Graduate Student	Male	Non-Hispanic	Caucasian	No
Alex Mastrean	Testing/Quality Engineer	Inactive June ‘16	Undergraduate	Male	Non-Hispanic	Caucasian	No
Srinidhi Ravi	Science Lead	Inactive July ‘16	Undergraduate	Female	Non-Hispanic	Asian Indian	No
Cheyenne Howard	Science Team	Inactive May ‘16	Undergraduate	Female	Non-Hispanic	Caucasian	No
Jia Zhuang	Communications Engineer	Inactive May ‘16	Undergraduate	Female	Non-Hispanic	Asian	No
John Stone	Support Engineer	Inactive May ‘16	Undergraduate	Male	Non-Hispanic	Caucasian	No
Kelly Johnson	Thermal Engineer	Inactive May ‘16	Undergraduate	Female	Non-Hispanic	Caucasian	No
Nathan Wilson	Support Engineer	Inactive May ‘16	Undergraduate	Male	Non-Hispanic	Caucasian	No
Stone Hanlon	Power Engineer	Inactive May ‘16	Undergraduate	Male	Non-Hispanic	Caucasian	No
James Cornelison	Graduate TA	Inactive May ‘16	Graduate Student	Male	Non-Hispanic	Caucasian	No
Candace Ashley	Science Team	Inactive January ‘16	Undergraduate	Female	Non-Hispanic	Caucasian	No
Jekan Thangavelautham	Faculty Advisor	Inactive January ‘16	Professor	Male	Non-Hispanic	Asian Indian	No
Erik Asphaug	Faculty Advisor	Inactive January ‘16	Professor	Male	Non-Hispanic	Caucasian	No

HIDRA Team Graduation Information

Name	Graduation Date	Degree	Current Status
John McCulloch	May 2016	Earth & Space Exploration, B.S.	Graduate student in Systems Engineering at Arizona State University's School of Computing, Informatics, and Decision Systems Engineering.
Bradley Karas	May 2016	Earth & Space Exploration, B.S.	Non-degree seeking graduate student at Arizona State University and Research Technician for ASU's Lunar Reconnaissance Orbiter Camera.
Nijiel Rocha	May 2016	Earth & Space Exploration, B.S.	Entered industry.
Alex Mastrean	May 2016	Earth & Space Exploration, B.S.	Graduate student in Astronautical/Aeronautical Engineering (Propulsion) at Purdue University.
John Stone	May 2016	Earth & Space Exploration, B.S.	Information unavailable.
Kelly Johnson	May 2016	Earth & Space Exploration, B.S.	Information unavailable.
Nathan Wilson	May 2016	Earth & Space Exploration, B.S.	Midshipman in the United States Navy.
Stone Hanlon	May 2016	Earth & Space Exploration, B.S.	Information unavailable.

Acknowledgements

Christopher Groppi, Professor (HIDRA Faculty Advisor)
School of Earth and Space Exploration, Arizona State University

Dr. Lindy Elkins-Tanton, Director
School of Earth and Space Exploration, Arizona State University

Paul Scowen, Professor
School of Earth and Space Exploration, Arizona State University

Andrew Thoesen, Ph.D Candidate
School of Earth and Space Exploration, Arizona State University

Outreach Efforts

As the HIDRA mission is part of the School of Earth and Space Exploration (SESE) at ASU, the HIDRA team took part in SESE's annual, educational outreach initiative called Earth and Space Exploration Day (ESE Day) on November 5, 2016. A description of ESE Day taken from its Facebook page is as follows:

> Earth and Space Exploration (ESE) Day is a free annual fall event hosted by the School of Earth and Space Exploration (SESE) on ASU's Tempe campus. The SESE community offers special science-related activities from 9 a.m.-3 p.m. for students age five and up, families, educators and anyone interested in exploring Earth and space. More than 40 exhibitors participated in the annual Earth and Space Exploration Day.

The HIDRA team's exhibit consisted of two flat-panel monitors showing the HASP launch video and a timelapse of the synced up visual and thermal images taken by HIDRA. In addition to the videos, the HIDRA team had a flyer with information regarding the mission to hand out to those who were interested. Many attendees were very interested in the project and some even asked how they could donate to fund future ASU payloads for HASP missions. A copy of the flyer is attached (front and back).

HIDRA Mission Summary

HIDRA (High-altitude Infrared Device for Research and Analysis) is a payload designed and built by students in ASU's School of Earth and Space Exploration for the HASP mission.

Launched from Fort Sumner, NM on Sept. 1, 2016 and at float at 120,000 ft. for approximately 15 hours, data from the HIDRA payload at float is currently being analyzed in furtherance of the scientific goals below. All indications from telemetry data indicate that HIDRA had a smooth flight with no anomalous behavior.

Scientific Goals:

Goal 1: Study the effects of human development on the local environments by taking thermal images in the 7-13 μm range and comparing the areas surrounding developed land to similar non-developed land.

Goal 2: Overlay thermal images on the USGS's National Land Cover Database to map specific temperature variations according to land cover type.

What is HASP?

The High Altitude Student Platform and is program run through NASA's BPO in partnership with the Louisiana Space Consortium to provide undergraduate and graduate students with the opportunity to design and build a high altitude balloon payload to conduct their experiments.

HIDRA

High-altitude Infrared Device for Research and Analysis

The HIDRA System

At its most basic level, the HIDRA payload consists of a FLIR infrared camera, a visual camera, and a command and control system housed in a 5.3" x 5.3" x 8.5" aluminum case with a total payload weight of 2.4 kg. The aluminum frame is secured to a PVC mounting plate provided by HASP and then the mounting plate is integrated on an exterior PVC arm of the HASP gondola and supplied ~28V power and data connectivity through an EDAC 516 connector and a DB9 serial connector, respectively.

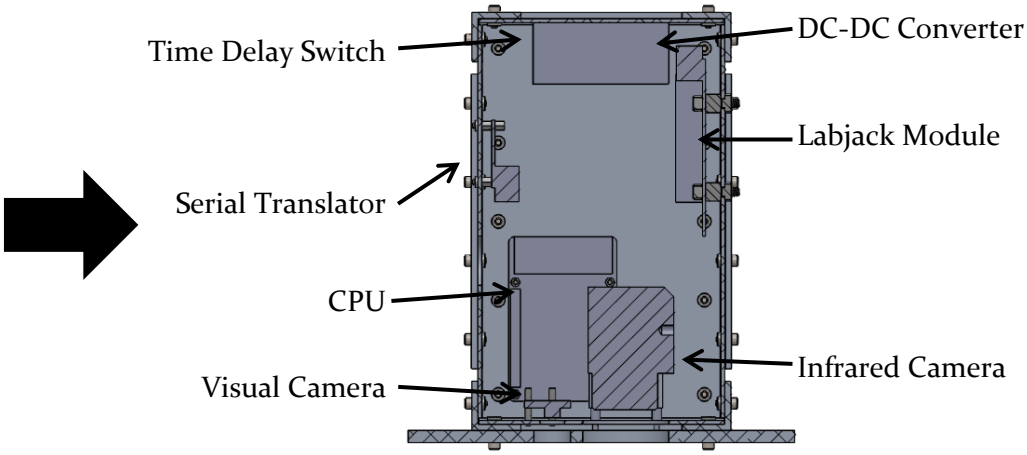

Visual and Infrared Imagery

The two images to the left are example images collected above the same area by HIDRA. The field of view of the visual image is larger than that of the infrared image and is used to identify geographic features in the infrared images. By linking common points in infrared images, and using the measured temperature of the airport tarmac from image IR0072, the pixel values of the infrared images can be adjusted to reflect an approximate temperature value to potentially provide quantitative as well as qualitative data for analysis in furtherance of the scientific objectives.

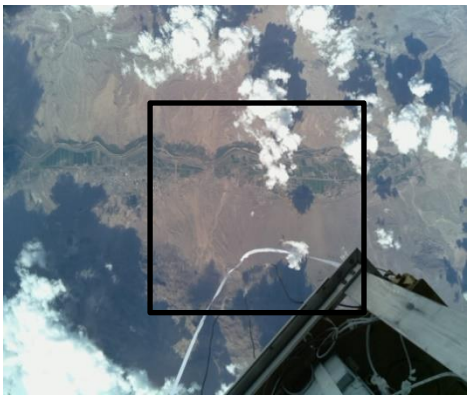

Visual Image

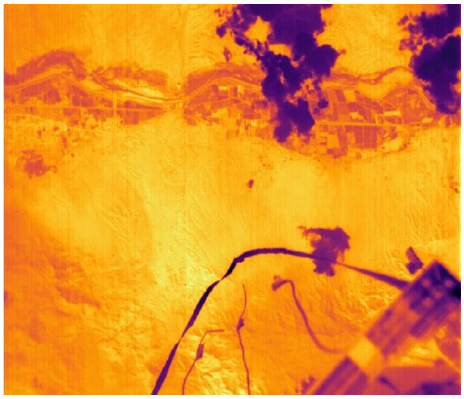

Infrared Image

HIDRA Team

Name	Role(s)	Student Status
John McCulloch	Systems Engineer Project Manager Power Systems Engineer	Graduate Student
Bradley Karas	Mechanical Engineer Camera Systems Engineer Scientific Analysis Lead	Graduate Student
Jacob Trahan	Computer Systems Engineer Communication Engineer	Undergraduate Student
Nijiel Rocha	Support Engineer – Thermal Systems, Calibration, & Assembly	Undergraduate Student
Akshay Vijay	Support Engineer – Testing, Machining	Undergraduate Student

L-R: Akshay Vijay, Jacob Trahan, John McCulloch, Bradley Karas, & Nijiel Rocha

ASU School of Earth & Space Exploration
Arizona State University